

# Structural, optoelectronic and electrochemical properties of nickel oxide films

B. Subramanian · M. Mohammed Ibrahim ·  
K. R. Murali · V. S. Vidhya · C. Sanjeeviraja ·  
M. Jayachandran

Received: 27 May 2008 / Accepted: 22 October 2008 / Published online: 13 November 2008  
© Springer Science+Business Media, LLC 2008

**Abstract** Thin nickel oxide (NiO) films were deposited by the electron beam evaporation technique. The films were post annealed in air at 450–500 °C for 5 h and the effect of annealing on the structural, microstructural, electrical and optical properties were studied. X-ray diffraction studies indicated the polycrystalline nature of the films. The microstructural parameters were evaluated. The band gap of the films was found to be about 3.60 eV. Electrical resistivity of the films was  $4.5 \times 10^{-4} \Omega \text{ cm}$ . FTIR studies indicated a broad spectrum centered at  $461.6 \text{ cm}^{-1}$ . Cyclic voltammetry studies in 1 M KOH solution revealed good electronic electrochromic behaviour.

## 1 Introduction

Among the numerous organic and inorganic electrochromic materials, the transition metal oxides are well studied because they show considerable variation in stoichiometry. Nickel oxide (NiO) is an anodic electrochromic material

(EC), which colours upon reduction (ion extraction). The phenomenon of anodic colouration of NiO allows potential applications of this material as a counter electrode in conjunction with tungsten oxide as working electrode in assembling EC devices. This has the advantage of increasing the optical density variation of the device, since the electrode colours and bleaches simultaneously [1]. Bulk NiO has a cubic (NaCl-type) structure with a lattice parameter of 0.4195 nm. It is considered to be a model semiconductor with hole-type conductivity. The stoichiometry of NiO is roughly indicated by the colour of the sample [2]. The colour of NiO is highly sensitive to the presence of higher valence states of nickel even in traces. The nickel cation vacancies and or interstitial oxygen in NiO crystallites results in non-stoichiometric  $\text{NiO}_x$ . NiO is a p-type semiconductor having wide band gap energy from 3.5 to 4.0 eV [2], although stoichiometric NiO is an insulator with resistivity of the order of  $10^{13} \Omega \text{ cm}$  at room temperature. It is an insulator due to Mott-type correlation of 3d electrons and does not show thermally induced Mott-transition. It is highly resistant to oxidation. The excellent chemical stability coupled with the interesting optical, electrical and magnetic properties make NiO as an excellent candidate for electrochromic devices [3]. Besides this, it is also a promising material for applications like smart windows, active optical fibers, gas sensors, solar thermal absorbers, catalyst for CO oxidation, fuel cell electrodes and photo electrolysis. Several techniques like sputtering [4], vacuum evaporation [5], electron beam evaporation [6], spray pyrolysis [2], chemical deposition [7], sol gel [8], pulse laser deposition [9] and plasma enhanced chemical vapour deposition [10] have been employed for the deposition of NiO thin films. It is well known that the structural properties and surface morphology of materials in thin film form depend on the deposition conditions and post

---

B. Subramanian · K. R. Murali · V. S. Vidhya ·  
M. Jayachandran (✉)  
Electrochemical Materials Science Division, Central  
Electrochemical Research Institute, Karaikudi 630006,  
Tamilnadu, India  
e-mail: jayam54@yahoo.com

M. Mohammed Ibrahim  
Birla Institute of Technology and Science (BITS)-Pilani,  
Dubai, UAE

C. Sanjeeviraja  
School of Physics, Alagappa University, Karaikudi 630003,  
Tamilnadu, India

deposition annealing. In this work, the electron beam evaporation technique was used to deposit NiO films. The structure, morphology, electrical, optical and electrochromic properties of these films were studied.

## 2 Experimental techniques

NiO thin films were deposited on glass substrates using a HindHivac 12" MSPT electron beam evaporation system. A vacuum better than  $10^{-5}$  mbar was maintained during evaporation. Prior to deposition, the glass substrates were boiled in chromic acid, followed by washing in deionized water. The substrates were then cleaned with acetone using an ultrasonic cleaner. NiO pellet of 99.995% purity (Alfa Aesar) was used as the source. The deposition time was 10 min. Thickness of the films measured by gravimetry was  $0.32 \mu\text{m}$ . The films were characterized by X-ray diffraction (XRD) studies using an X'pert Pro PANanalytical X-ray diffractometer. Optical absorption spectra were recorded using a U 3400 UV-Vis-NIR spectrophotometer. Fourier transform infrared (FTIR) studies were conducted with Perkin Elmer system. Electrical conductivity measurements were made by the four-probe technique. Surface morphology was studied with a molecular imaging atomic force microscope (AFM) system. Electrochemical studies were made using a PARSTAT 2273 Advanced Electrochemical system.

## 3 Results and discussion

X-ray diffraction studies indicated weak NiO diffraction peaks corresponding to the (111), (200) and (220) orientations (Fig. 1). A broad peak around  $11^\circ$  due to  $\text{Ni}(\text{OH})_2$  is also observed. The films were post annealed at different temperatures in the range of  $400\text{--}500^\circ\text{C}$  in air to improve the crystallinity. No significant changes were observed beyond  $500^\circ\text{C}$ , hence the temperature range was restricted to  $500^\circ\text{C}$ . After post anneal at  $500^\circ\text{C}$ , the XRD pattern exhibited intense peaks corresponding to the (111) and (200) orientations of cubic NiO (JCPDS File no. 89-7130) (Fig. 2). The experimental data agrees well with the JCPDS data indicating the presence of NiO. The micro structural parameters, like, grain size, lattice parameter, strain and dislocation density were calculated and are presented in Tables 1 and 2 for the as-deposited films and for the films annealed at  $500^\circ\text{C}$ , respectively. The calculated lattice parameter values  $4.1904$  and  $4.1838 \text{ \AA}$  agree well with the standard value of  $4.1950 \text{ \AA}$  for FCC NiO phase [11].

The absorption spectrum of the NiO film annealed at  $500^\circ\text{C}$  was recorded in the wavelength range

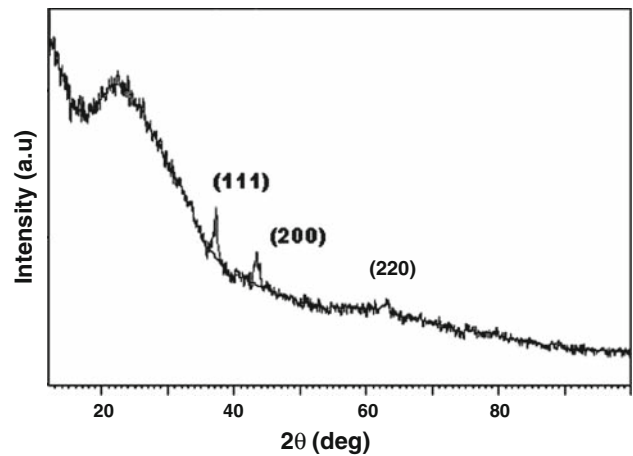


Fig. 1 XRD pattern of as-deposited NiO film

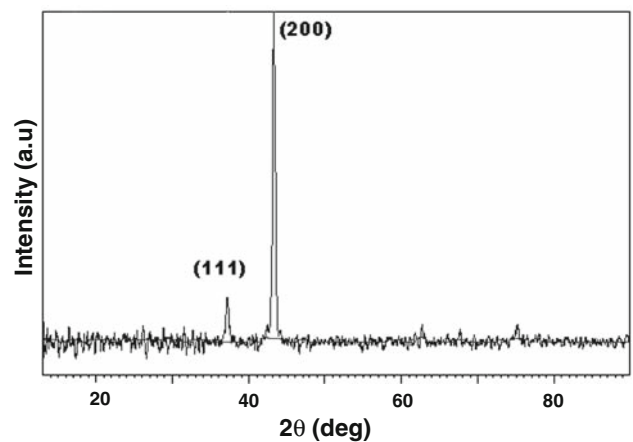


Fig. 2 XRD pattern of NiO film post annealed at  $500^\circ\text{C}$

$300\text{--}1000 \text{ nm}$  (Fig. 3), and the observed sharp decrease at about  $320 \text{ nm}$  may be attributed to the band edge absorption of NiO. The band gap of the film was estimated from the well known equation:

$$\alpha = A(h\nu - E_g)^n$$

where  $\alpha$  is the absorption coefficient and  $E_g$  is the band gap of the film. For a direct band-to-band allowed transition, the value of  $n = 1/2$ . A plot of  $(\alpha h\nu)^2$  versus  $h\nu$  (Fig. 4) yielded a straight line. Extrapolation of the line to the  $h\nu$  axis yielded a band gap of  $3.60 \text{ eV}$ . The reported band gap values for NiO films are in the range of  $3.15\text{--}3.80 \text{ eV}$  [12, 13].

Surface morphology of the film was studied by AFM. Figure 5a shows the 2D and 3D topography of the as-deposited NiO film. Figure 5b shows the 2D and 3D topography of the NiO film post heat treated at  $500^\circ\text{C}$ . Presence of hillocks are observed on the surface. As the annealing temperature is increased to  $500^\circ\text{C}$ , the number of hillocks are found to decrease and the surface becomes

**Table 1** Microstructural parameters of as-deposited electron beam evaporated NiO films

Lattice parameter a (Å)	d-spacing observed (Å)	d-spacing standard (Å)	d(hkl)	Grain size D (nm)	Strain $\epsilon \times 10^{-3}$ (line <sup>-2</sup> m <sup>-4</sup> )	Dislocation density, $\delta \times 10^{16}$ (line m <sup>-1</sup> )
4.1904	2.4247	2.4216	(111)	26.36	1.112	1.508
	2.0952	2.0972	(200)	28.19	0.883	1.115
	1.4848	1.4892	(220)	29.13	0.614	0.765

**Table 2** Microstructural parameters of electron beam evaporated NiO films annealed at 500 °C

Lattice parameter a (Å)	d-spacing observed (Å)	d-spacing standard (Å)	d(hkl)	Grain size D (nm)	Strain $\epsilon \times 10^{-3}$ (line <sup>-2</sup> m <sup>-4</sup> )	Dislocation density, $\delta \times 10^{16}$ (line m <sup>-1</sup> )
4.1838	2.4171	2.4216	(111)	16.359	1.772	3.881
	2.0919	2.0972	(200)	23.031	1.090	1.697

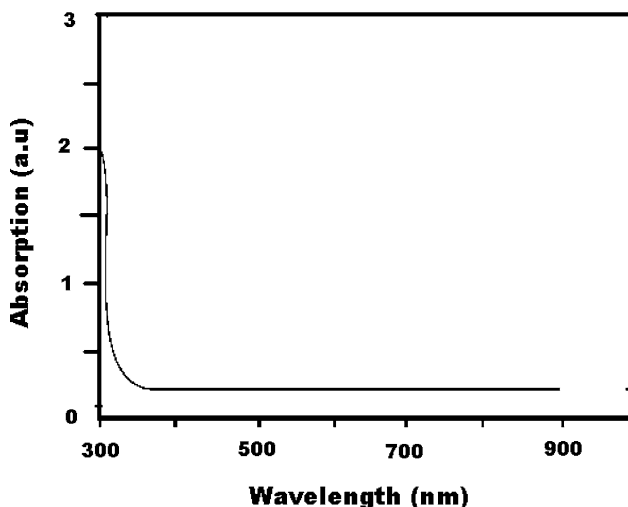


**Fig. 3** Absorption spectrum of NiO film

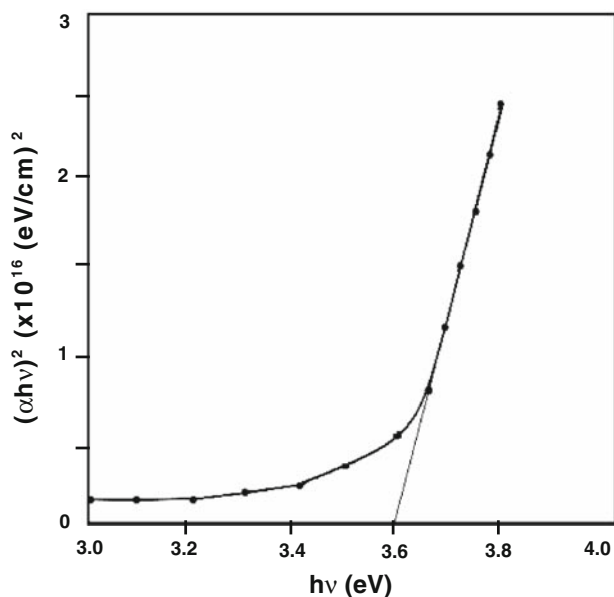


**Fig. 4**  $(\alpha hv)^2$  versus  $h\nu$  plot of NiO film

smooth (Fig. 5b). The surface roughness decreases from 20 to 10 nm after heat treatment at 500 °C.

Resistivity of the films was measured by the four probe method using the standard relation

$$\rho = 4.532 \times (V/I) \times t$$

where  $\rho$  is the resistivity, V is the applied voltage and I is the current, t is the film thickness. The value of resistivity is  $4.5 \times 10^{-4} \Omega \text{ cm}$ . The conduction mechanism of the NiO film is associated with the vacancies existing in the structure. The electrical properties of NiO films are depend on their microstructure and composition, and consequently on the deposition environment [14–17]. Non-stoichiometric NiO is known as a p-type extrinsic semiconductor [12]. The defects which are the cause for hole conductivity in NiO are Ni<sup>2+</sup> ion vacancies. Each vacancy is filled with two Ni<sup>3+</sup> ions, which can act as electron acceptors. However, crystalline NiO film showing (200) orientation is formed with near stoichiometric ratio. Highly stoichiometric NiO is an insulator with high resistivity ( $\rho > 10^{13} \Omega \text{ cm}$ ) at ambient temperature. In the present study, the NiO films were found oriented along (111) and (200) directions. The resistivity value obtained in this work is very much less than the values reported earlier [18]. The observed lower resistivity values obtained in this work may be due to the fact that post annealing of the NiO films might have brought about non-stoichiometry.

Figure 6 shows the FTIR transmission spectra of the NiO film. The spectrum exhibits a broad peak in the region of 450–470 cm<sup>-1</sup>. The peak attains maximum at 461.02 cm<sup>-1</sup> which corresponds to the Ni–O stretching vibration [19].

Figure 7 shows the cyclic voltammograms (CVs) recorded in 1 M KOH electrolyte. Typical CV spectra were recorded for different cycles (100–500 cycles in steps of 50 cycles) in the potential range –0.2 to 0.7 V versus SCE at a scan rate of 50 mV/s. As the cycle increases, the voltammograms are shifted towards right with a corresponding

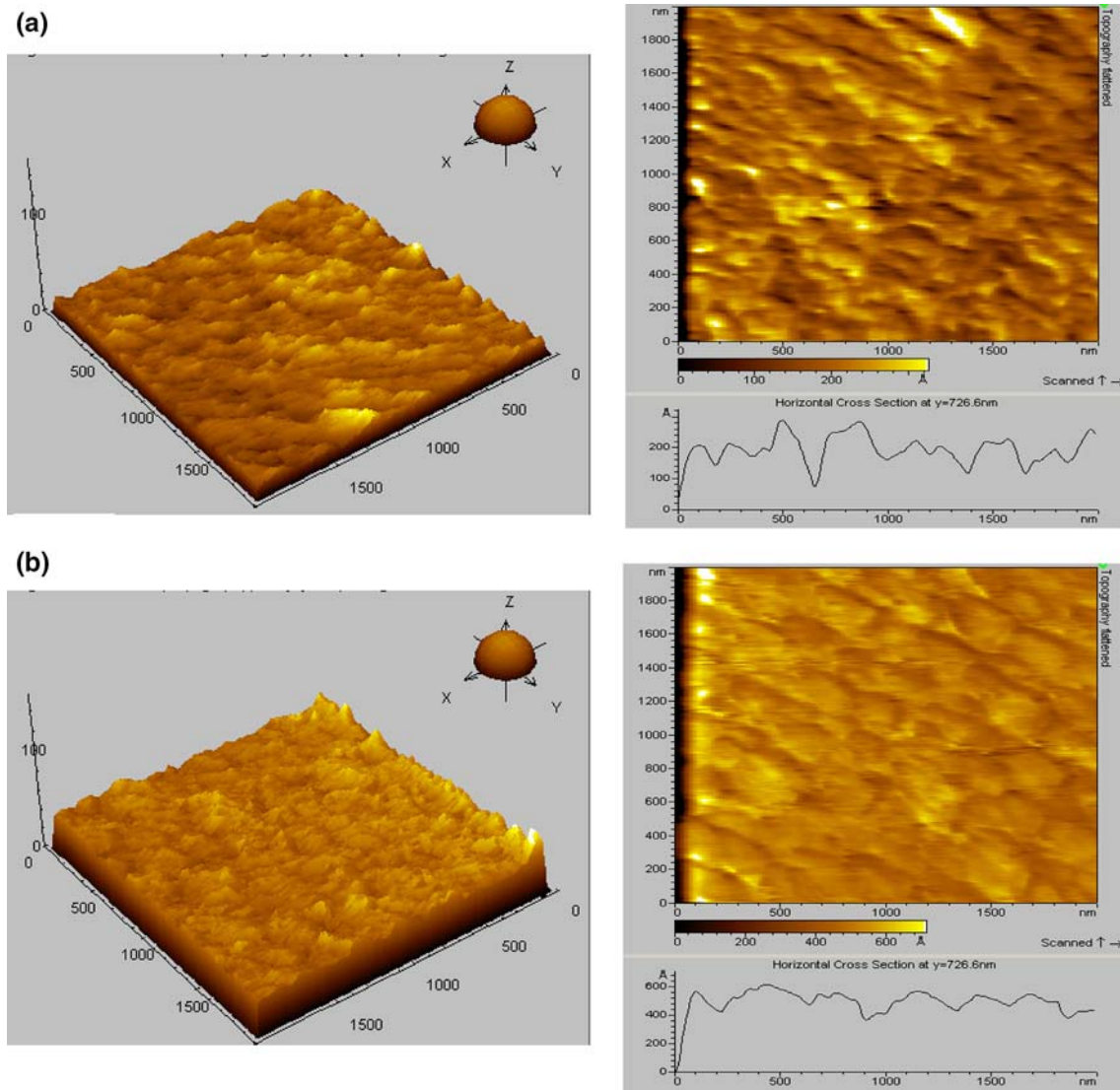


Fig. 5 Surface morphology of the **a** as-deposited NiO film and **b** NiO film post annealed at 500 °C

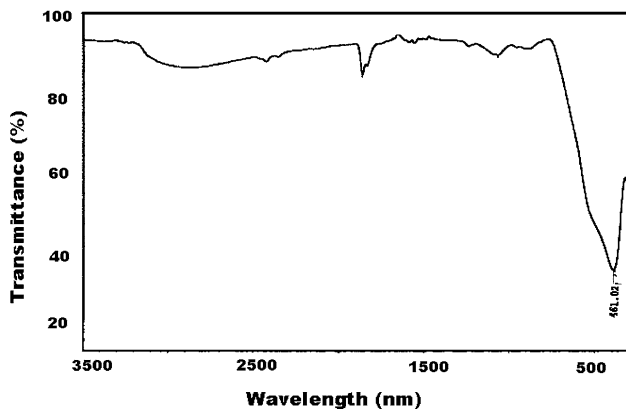


Fig. 6 FTIR spectrum of NiO film post annealed at 500 °C

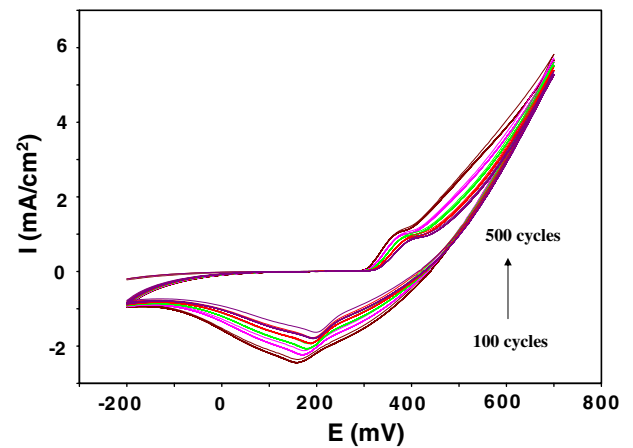
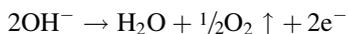
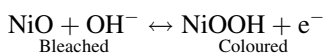


Fig. 7 Cyclic voltammograms of NiO films for different cycles

increase in potential and decrease in current. This is due to the degradation associated with increasing porosity of the NiO working electrode. During the anodic scan, i.e. scanning from  $-0.2$  to  $0.7$  V, current remains practically zero up to about  $350$  mV and then it increases sharply due to the oxidation of Ni(II) to Ni(III) producing a deep brown colouration in the film. The steep increase in current recorded at the end of anodic sweep is due to the oxygen evolution reaction according to the following reaction:



During the cathodic scan, scanning the voltage from  $0.7$  to  $-0.2$  V, cathodic peaks are observed between  $200$  and  $155$  mV (SCE) causing bleaching of the film. Colouration and bleaching process is accompanied with insertion and deinsertion of  $\text{OH}^-$  ions and electrons in the NiO film. In this way, all the NiO films show anodic colouration (brown) and cathodic bleaching (colourless) according to the following electrochemical reaction,



The process of colouration and bleaching in nickel oxide film occurs by the extraction/insertion of 3d electrons [20] without affecting the metal-oxygen bond. The top of the valence band of nickel oxide consist of nickel 3d states [21] in contrast to the oxygen 2p states present for most other oxides. Hence, no fundamental requirements needed for the nickel oxide films to be hydrogen containing in order to possess electrochromic properties. Coloured states correspond to partially filled valence band or, in other words, presence of electron vacancies on nickel atoms. In the bleached state, the valence band is completely filled. This colouration mechanism is consistent with the p-type conductivity reported for NiO containing excess oxygen [22]. The deep brown colouration of the NiO film is associated with the oxidation peak observed prior to current increase due to oxygen evolution, whereas the bleaching process is associated with the cathodic reduction peak which is in accordance with the reported anodic electrochromism in nickel oxide films [23].

#### 4 Conclusion

The results of this investigation clearly demonstrate that low resistivity NiO films, possessing anodic electrochromic properties, can be easily deposited by the electron beam evaporation technique. The less crystalline NiO film was

changed to have highly crystalline nature with FCC structure, after annealing the sample at  $500$  °C. Uniform surface morphology with fine grain structure was evident from AFM analysis. The anodic color change of the NiO film, from transparent to brown color, was observed by cyclic voltammetric studies.

#### References

1. S.A. Mohammed, A.A. Atel, H. Kamal, K. Abdal-Hady, *Physica B* **311**, 366 (2002)
2. J.D. Desai, S.K. Min, K.-D. Jung, O.-S. Joo, *Appl. Surf. Sci.* **253**, 1781 (2006)
3. M. Kitao, K. Izawa, K. Urabe, T. Komatsu, S. Kuwano, S. Yamada, *Jpn. J. Appl. Phys.* **33**, 6656 (1994)
4. H.Y. Ryu, G.P. Choi, W.S. Lee, J.S. Park, *J. Mater. Sci. Lett.* **39**, 4375 (2004)
5. B. Sasi, K.G. Gopachandran, P.K. Manoj, P. Koshy, P. Prabhakara Rao, V.K. Vaidyan, *Vacuum* **68**, 211 (2002)
6. A. Agarwal, H.R. Habibi, R.K. Agarwal, J.P. Cronin, D.M. Roberts, C.P. R'Sue, C.M. Lampert, *Thin Solid Films* **221**, 239 (1992)
7. M.A. Vidales-Hurtado, A. Mendoza-Galvan, *Mater. Chem. Phys.* **107**, 33 (2008)
8. R.C. Korosec, P. Bukovec, *Acta Chim. Slo.* **53**, 136 (2006)
9. M. Tanaka, M. Mukai, Y. Fujimori, M. Kondoh, Y. Tasaka, H. Baba, S. Usami, *Thin Solid Films* **281–282**, 453 (1996)
10. E. Fujii, A. Tomozawa, S. Fujii, H. Torii, M. Hattori, R. Takayama, *Jpn. J. Appl. Phys.* **32**, L1448 (1993)
11. I. Hotovy, D. Buc, S. Hascik, O. Nennewitz, *Vacuum* **50**, 41 (1998)
12. H. Suto, T. Minami, S. Takata, T. Yamada, *Thin Solid Films* **236**, 27 (1993)
13. P. Puspharajah, S. Radhakrishna, A.K. Aroif, *J. Mater. Sci.* **32**, 3001 (1997)
14. O. Kohmoto, H. Nakagawa, F. Ono, A. Chayahara, *J. Magn. Mater.* **226–230**, 1627 (2001)
15. Y.M. Lu, W.S. Hwang, J.S. Yang, *Surf. Coat. Technol.* **155**, 231 (2002)
16. H.L. Chen, Y.M. Lu, W.S. Hwang, *Surf. Coat. Technol.* **198**, 138 (2005)
17. H.L. Chen, Y.M. Lu, W.S. Hwang, *Thin Solid Films* **514**, 361 (2006)
18. H.L. Chen, Y. Sheng Yang, *Thin Solid Films* **516**, 5590 (2007)
19. R.C. Korosec, P. Bukovec, B. Pilhar, A. Surca Vuk, B. Orel, G. Drazic, *Solid State Ionics* **165**, 191 (2003)
20. A. Azena, L. Kullman, G. Vaivars, H. Nardberg, C.G. Granquist, *Solid State Ionics* **113**, 449 (1988)
21. J. Hugal, M. Kamal, *J. Phys. Condens. Mater.* **9**, 647 (1997)
22. E. Iguchi, K. Akashi, *J. Phys. Soc. Jpn.* **61**, 3385 (1992)
23. J.I. Garcia Miquel, Q. Zhang, S.J. Allen, A. Rougier, A. Blyc, H.O. Davies, A.C. Jones, T.J. Leedham, P. Williams, S.A. Impey, *Thin Solid Films* **434**, 165 (2003)